Pakistan Veterinary Journal

ISSN: 0253-8318 (PRINT), 2074-7764 (ONLINE)
DOI: 10.29261/pakvetj/2025.282

RESEARCH ARTICLE

Triton X-100 - Coated Toltrazuril Nanoparticles: A Promising Anti-Coccidial Formula for Effective Treatment of Poultry Coccidiosis

Shiem El-Sherry[1*]; Asmaa Nasr[2] and Gamal Zayed[3,4]

[1]Department of Avian and rabbit medicine, Faculty of Veterinary Medicine, Assiut University, Assiut, 71526, Egypt; [2]Poultry diseases department, Animal Health Research Institute, Assiut regional laboratory, Agricultural research center, Assiut, Egypt; [3]Dept. of Pharmaceutics and Pharmaceutical Technology, Faculty of Pharmacy, Al-Azhar University, Assiut, Egypt; [4]Al-Azhar Center of Nano-sciences and Applications (ACNA), Al-Azhar University, Assiut, Egypt.
*Corresponding author: shiemelsherry@aun.edu.eg

ARTICLE HISTORY (25-314)

Received: April 13, 2025
Revised: September 06, 2025
Accepted: September 07, 2025
Published online: October 16, 2025

Key words:
Avian coccidiosis
Triazinetrione
Nano-formula
Solvent anti-solvent
Eimeria tenella
ISI approach

A B S T R A C T

Toltrazuril, a triazinetrione derivative, is still one of the most effective antiparasitic drugs used to treat coccidiosis. However, the drug has some limitations, including the emergence of resistance and poor aqueous solubility. The study's objective was to develop coated toltrazuril nanoparticles to improve toltrazuril solubility and drug efficacy. Different nano-toltrazuril formulations were prepared using the "solvent-anti-solvent" technique, utilizing different concentrations of surfactants and raw material. Toltrazuril nanoparticles coated with triton X-100 were optimized and characterized in terms of size, polydispersity index and by TEM imaging. The efficiency of the new formula was examined in vivo using 80 broiler chickens infected with *Eimeria tenella* oocysts. Dynamic light scattering (DLS) revealed that the obtained nanoparticles had a homogeneous size and distribution (average 152.7 nm) and a polydispersity index less than 0.7. TEM measurements revealed nanoparticles with quasi-spherical shapes and particle sizes (13 nm by 47 nm). At room temperature, toltrazuril nanoparticles sustained dispersion stability for 7 months. Toltrazuril nanoparticles (1.3 mg/kg B.W.) in drinking water enhanced anticoccidial efficacy compared to the reference dosage (10 mg/kg B.W.) in *Eimeria tenella* -infected chickens. Toltrazuril nano-form significantly reduced oocyst output ($0.6 \pm 2.4 \times 10^6$) less than the reference dose ($24.5 \pm 9.6 \times 10^6$). The histological (I See Inside) approach revealed a significant improvement in microscopic cecal lesion scores in nano-toltrazuril-treated birds (22) compared to commercial toltrazuril-treated birds (45). The survival rate of birds had also increased. In conclusion, the selected toltrazuril nano formula effectively increased the drug's solubility and stability, and a significant improvement in performance metrics was observed.

To Cite This Article: EL-Sherry S; Nasr A and Zayed G 2025. Triton X-100 -coated toltrazuril nanoparticles: a promising anti-coccidial formula for effective treatment of poultry coccidiosis. Pak Vet J. http://dx.doi.org/10.29261/pakvetj/2025.282

INTRODUCTION

Chicken coccidiosis is directly to blame for a global loss of £10.4 billion (Blake *et al.,* 2020). One or more of seven Eimeria species are reported to induce severe enteritis in chickens, but *Eimeria tenella (E. tenella*) is the most pathogenic species and one of the most frequently reported *Eimeria species* in broiler chickens (Blake *et al.,* 2020). Infection with *Eimeria spp.* diminishes cecal health, resulting in decreased feed competence and small intestinal health in broilers. Chicken cecum is the main site for volatile fatty acids production and diverse pathogens` house. Control methods are mostly reliant on vaccination and chemotherapy (Burrell et al., 2020; Zaheer *et al.*, 2022). Chemotherapeutic anticoccidial therapies remain the most effective approach for coccidiosis control. However, anticoccidial drugs face major challenges that limit their efficacy, such as the development of parasitic resistance. Furthermore, few new treatments have been introduced, and new chemotherapeutics are unlikely to be developed (Mustafa *et al.*, 2025) . Recent research trends demonstrate growing interest in exploring phytotherapeutic alternatives such as essential oil or herbal extracts for avian coccidiosis, with promising efficacy and enhanced safety compared to conventional treatments (Saeed *et al.,* 2023).

Additionally, nano-formulations have emonstrated remarkable success across various medical treatments (Mustafa *et al.,* 2025). Metal-based nanoparticles (NPs) represent unique physicochemical properties, including high surface area, homogenous morphology, and biocompatibility. Different metals like gold (Au), silver (Ag), iron oxide (Fe_3O_4), zinc oxide (ZnO), and titanium dioxide (TiO_2) are extensively used in diverse medical applications from parasites treatments to protection against cancer (Harron *et al., 2024*). Emerging approaches that combined nanotechnology with green chemistry are proving more rewarding, offering dual advantages of enhanced efficiency and greater safety. Green synthesized iron-oxide nanoparticles using *Ficus racemosa* Linn leaf extract induced fast recovery and growth enhancement in *E. tenella* infected broilers (Khan *et al., 2023*). Nanotechnology unlocks new possibilities for reformulating chemotherapy drugs by boosting efficiency, reducing costs, and improving safety (El-Sawah *et al,* 2024). Toltrazuril, a water-insoluble triazinetrione derivative, is one of the most effective anticoccidial agents against all *Eimeria spp*. However, the reduced sensitivity of *Eimeria spp.* to toltrazuril was recorded (Sun *et al.,* 2023). The bioavailability of water-insoluble drugs can be increased as particle size is reduced. One of the promising methods for producing stable and small-sized nanoparticles with reduced crystallinity is the solvent-anti-solvent precipitation technique. Polymers (Polyvinylpyrrolidone and Polyethylene Glycol), nonionic surfactants, and co-surfactants (pluronic F127) have all been successfully used in the stabilization of nanoparticles (Pouretedal *et al.,* 2014; Wu *et al.,* 2022). Few attempts to modify the formulation of toltrazuril have been effectively tested using lipid core nanoparticles or nanomicelle delivery systems (Baron *et al.,* 2022; Zhang *et al.,* 2018). Even with only half the medication concentration utilized in commercial formulations, several formulations were able to produce similar significant effects (Zhang *et al.,* 2018). A quarter dose of nanoemulsion of diclazuril achieved similar efficacy to 10 mg/mL diclazuril while maintaining diclazuril's established safety profile in treated chicks (El-Sawah *et al,* 2024).

The current study attempted to develop small, stable toltrazuril nanoparticles to improve the drug's aqueous solubility and bioavailability. Various surfactants, such as tween 80, span 80, sodium deoxycholate (NaDC), and triton X-100, had been investigated as stabilizers. The effect of stabilizer concentrations, drug concentrations, and dripping rate on particle size was reported. The in vivo activities of nano-precipitated toltrazuril were compared to those of commercial toltrazuril.

MATERIALS AND METHODS

Preparation of toltrazuril nanoparticles (TLZ-NPs): The solvent-anti-solvent technique (Wu *et al.,* 2022) was applied using absolute ethanol as a solvent and water as an antisolvent. Different stabilizers (tween 80, span 80, NaDC, and triton X-100) had been used (Rohm and Hass® Co., Lobachemie, Germany). 30 ml of toltrazuril-ethanol solution (Ubei Long Xiang Pharmaceutical,Tech. Co., Ltd., China) was prepared (0.17, 0.8, and 1.5 mg/ml, respectively). Drug solutions were injected at two injection rates (50 µl/second and 200 µl/second) into a 100 ml watery surfactant solution with stirring (2500 rpm) (Table 1). Stirring continued for two hours to ensure ethanol evaporation. TLZ-NPs were centrifuged at 16000 xg for 30 min., precipitates were washed twice, dried in desiccators, and stored.

Characterization of the prepared formulas: Multilevel full factorial design, using Statgraphics XVII-X64 software, was adapted to optimize the preparation of triton X stabilized-toltrazuril nanoparticles. The independent variables (factors) for the optimization (Table 2) were the drug concentration (X1), triton X concentrations (X2) and the rate of drug injection (X3). The study evaluated how three independent variables affected the selected response characteristics, specifically nanoparticle size (Y_1) and size distribution (Y_2, PDI). Particle size and distribution were determined using Zetasizer ZS 90 (Malvern Nano Zetasizer, Germany). The samples were diluted by purified water to 0.2 mg/ml, and the size was measured (Ahmed *et al.,* 2016). Fourier transform infrared spectroscopy (FTIR) (Nicolet 6700 FTIR, Shimadzu Co., Japan) was used to record the FTIR spectrum of formulas. Samples were mixed with potassium bromide (KBr) powder, pressed to form hard disks, and scanned from 4000 to 400 cm^{-1} (Ahmed *et al.,* 2016). The crystallinity of the obtained TLZ-NPs was confirmed by powder X-ray diffraction XRD which carried out at a scanning rate 0.600 degree/min. over a 2-theta (4 to 60 degree). Morphology and the average particles size were determined using an electron microscope (JEOL JEM-100CX II Electron Microscope, Japan). Approximately 200 particles were measured (Baron *et al.,* 2022). TLZ-NPs were stored in a dark container at 28-32ºC with RH of 60-65%. The size and polydispersity index (PDI) were determined from the agitated samples monthly using Zetasizer for 7 months (Baron *et al.,* 2022). The production efficacy (PE) of TLZ-NPs was determined as follows: 3 ml were cold centrifuged at 15000 rpm for 30 min. Precipitated TLZ-NPs were washed, vacuum dried at 60 °C and weighted to ensure complete vaporization of water. 10 mg was dissolved in ethanol, and the concentration was determined by a UV-vis spectrophotometer at λmax 242 nm. Production efficiency was computed using the equation (El-Feky *et al.,* 2013).

$$PE\ \% = \frac{\text{Weight of drug in nanoparticles}}{\text{Initial weight of drug}} \times 100$$

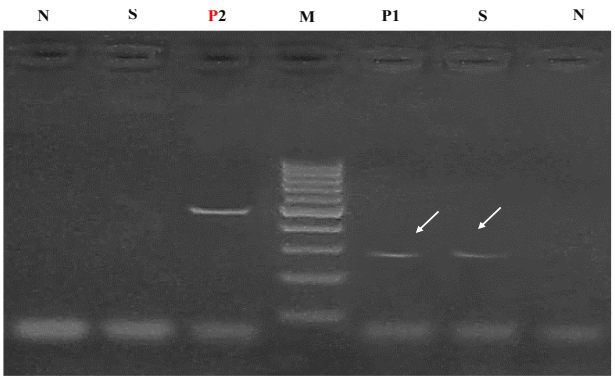

Fig. 1: Agarose gel electrophoresis image showing the amplified internal transcribed spacer of nuclear rDNA gene (*ITS*) of the *Eimeria* spp. Lane P1: Positive control for *E. tenella* (amplicon size 278 bp); Lane P2: Positive control for *E. maxima* (505 bp); Lane M: 1000 bp DNA marker; Lane N: Negative control (No band); Lane S: the experimental sample displaying amplicon size 278 bp specific to *E. tenella* but negative to *E. maxima.*

Table 1: Effect of different types and concentration of stabilizers. and toltrazuril on nano-particle size distribution and Polydispersity index

Injection speed (µl/min)	drug conc. (mg/ml)	Surf. conc. (w/v)	Particle size distribution (PSD) (nm)				Polydispersity index (PDI)			
			Tween 80	NaDC	Span 80	Triton x100	Tween 80	NaDC	Span 80	Triton x100
200	1.5	0.25	0	0	1083	2210	0.055	0.283	0.809	0.276
50			0	783.9	499.9	------	1	0.625	0.074	----
200	0.8		0	2899	734.7	887.5	1	0.774	0.525	0.014
50			0	415	341.4	421.2	1	0.824	0.105	1
200	0.17		0	1307	323.6	676.9	1	0.413	0.406	0.18
50			0	743.4	288.5	368.3	1	0.029	0.26	0.515
200	1.5	0.5	6908	0	220.8	2289	0.334	0.125	0.278	0.583
50			4454	751.3	202.9	755.6	0.266	0.543	0.198	0.319
200	0.8		1484	440.6	176.5	853.2	0.477	0.24	0.254	0.358
50			1202	352.5	149.8	325.6	0.316	1	0.126	1
200	0.17		535.6	259.2	159.9	458.7	0.784	1	0.226	0.063
50			91.28	13.54	152.7	152.7	0.417	0.739	0.156	0.312
200	1.5	1	0	2199	234.3	1742	1	0.354	0.392	0.544
50			594.3	513.6	269.1	497.3	0.671	0.972	0.408	1
200	0.8		0	452.9	225.7	493.5	1	1	0.245	1
50			1116	282.3	173.5	218.2	1	0.148	0.236	0.726
200	0.17		----	789.3	191.1	288.8		0.357	0.448	0.801
50			33.04	76.6	194.3	141.8	1	1	0.244	0.072

Table 2: Variables in multilevel full factorial design.

Independent variables, factors	Low	Medium	High
X1: Drug concentration (mg)	0.17	0.8	1.5
X2: Triton X concentrations (mg)	0.25	0.5	1
X3: Rate of drug injection (µl/min)	50	------	200

Dependent variables and responses; Y1: Particle size (nm)Y2: poly dispersity index

Parasites, birds, and experimental design: Infected cecal contents were collected and examined morphometrically for *E. tenella* identification using standard procedures (Mesa-Pineda *et al.,* 2021). A PCR primer pair for identification of *E. tenella* internal transcribed spacer of the nuclear rDNA gene (ITS) was used for confirmation (Lee *et al.,* 2010) (Fig.1). Oocysts were suspended in 2.5% potassium dichromate and sporulated by aeration (El-Sherry *et al.,* 2019). Eighty (one-day-old) broiler Ross chicks were purchased (Assiut for Investment and Development Co., Assiut, Egypt). All experiments were performed in experimental units of the avian and rabbit medicine department, faculty of veterinary medicine, Assiut University and were approved by the National Ethical Committee of the faculty of veterinary medicine, Assiut University, Assiut, Egypt, according to the OIE standards for the use of animals in research in accordance with ARRIVE guidelines. (reference no.06-2023-0030).

At 18 days old, birds were sorted randomly into four groups (20 birds per group): control, infected, infected and treated with Nalcoxi® (Toltrazuril, ATCO PHARMA, Assiut, Egypt), and infected and treated with TLZ-NPs. The recommended light and temperature program was used to raise the chicks in wire cages. Ad libitum food and water were given to the chicks. After being fed a broiler starter ration for 14 days, the birds were fed a grower diet. All birds except control were inoculated orally into the crop with 1.3 x 10^4 sporulated oocysts per bird. Drugs were administered 48 hrs. post-infection (10 mg/kg B.W. for toltrazuril) and (1.3 mg/kg B.W. for TLZ-NPs) using the TX-100 0.5% formula for two consecutive days. The survival rate was calculated at 7 days post-infection (surviving birds/initial birds) × 100. Drug efficacy was evaluated via oocysts output (El-Sherry *et al.,* 2019), and protection rate (the number of oocysts from infected unmedicated control − the number of oocysts from medicated) / the number of oocysts from infected unmedicated control ×100. (Belote *et al.*, 2019; Holdsworth *et al.,* 2004; Li *et al.,* 2023). Birds were euthanized by cervical dislocation. Macroscopic and microscopic cecal lesion scores were compared using the "I see inside" approach (Belote *et al.,* 2019). Briefly, an organ impact factor (OIF) is obtained from macroscopic Carcasses were systematically examined using a standardized protocol, divided into five anatomical areas: (1) locomotor system, (2) gastrointestinal tract (GIT)-associated organs, (3) intestinal tract, (4) coccidiosis-specific lesions, and (5) respiratory system. This methodological technique was designed to detect different organs relationships, with particular interactions between different systemic issues and intestinal health (Kraieski *et al,*2017). The microscopic analysis represents the reduction in organ functional capacity and ranging from 0-3. The intensity or frequency of the lesion is evaluated with a score (S) ranging from 0 to 3, depending on the percent of alteration that occurred in affected organ. The ISI total score was produced by multiplying the OIF of each alteration by its respective score number, and the results of all alterations are summed according to the formula ISI=S (OIF*S), where OIF=Organ impact factor and S=score (Belote *et al.,* 2019).

Statistical analyses: Data were analyzed by SPSS v26.0 using a one-way analysis of variance followed by Duncan's multiple range test. Data are the mean ± SD. A P value < 0.05 was considered statistically significant. Kruskal-Wallis analysis was employed for lesion scores (Holdsworth *et al.,* 2004; Li *et al.,* 2023).

RESULTS

Effects of different stabilizers, drug concentration, and instillation speed: Table (1). The decrease in drug concentration and injection speed led to a marked reduction in particle size. At a higher concentration and faster injection rate, numerous nuclei were formed and aggregated to form larger particles. The effect of drug concentration on PDI, interaction (AB), and quadratic effects (AA) (BB) is statistically insignificant (P>0.05) (Fig. 2).

The combined triton X-100 and toltrazuril produced the best formalized TLZ-NPs. Upon increasing triton X-100 from 0.25 mg to 1 mg, both the particle size and PDI of the obtained nanoparticles increased. The effect of triton X-100 concentration on particle size and PDI was statistically

significant (Fig. 3a). However, the interaction (AB) and quadratic (AA) (BB) effects are statistically insignificant (P>0.05) (Fig. 3b,c). The formula that was chosen to be evaluated *in vivo* consisted of 0.17 mg/ml toltrazuril with 0.5% triton x-100 average particle size of 152.7 nm. FTIR of TLZ-NPs showed the characteristic absorption peaks at wave numbers 3300, 2923, and 1585 cm^{-1}, the same as those of the raw drug (Fig. 4a). This finding confirms that TLZ-NPs retained its chemical structure with decreasing particle size and did not interact chemically with triton X-100. Toltrazuril showed many diffraction peaks in the 2θ range of 10-40 (Fig. 4b). The high-intensity peaks of the pure drug indicated a high-crystalline low energetic state. XRD of TLZ-NPs showed the complete disappearance of the drug's characteristic peaks, indicating the complete conversion of the drug to the high energetic amorphous state.

In TEM image Fig. 4c, formulated nanoparticles are nearly spherical in shape with almost uniform nanometric size (~13 to 47 nm). For distribution and PDI, the size of the suspended TLZ-NPs was slowly increased (about 40 nm monthly). Within 7 months, the particle size increased from 115.6 nm to 117.5 nm indicating very good dispersion stability (Fig. 5). 99.89% entrapment efficiency was obtained.

Effect of TLZ-NPs on *Eimeria tenella* infected chickens

Clinical features and survival rate: Chickens in the infected group exhibited severe signs of depression, bloody diarrhea, and mortalities. Symptoms decreased noticeably in both Nalcoxi group and the TLZ-NPs group. Survival rate was 40% in infected, 60% in the Nalcoxi group and 70% TLZ-NPs group.

Oocysts output: TLZ-NPs prominently reduced oocysts output to about 10 folds (0.6±2.4x 10^6 oocysts/gm fecal material) less than Nalcoxi (24.5±9.6 x 10^6 oocysts/gm fecal material) (Fig. 6a). Oocysts shedding decreased dramatically in treated groups compared to the infected-untreated group (32.2±10.2 x 10^6 oocysts/gm fecal material). The TLZ-NPs protection ratio amounted to 92.4 % while it was only 24.6% for the Nalcoxi group (Fig. 6b).

Macroscopic lesion score: In the TLZ-NPs group, a significant reduction (1.4±0.01) in the lesion score of the cecal mucosa was recorded (Fig. 6c). Nalcoxi group reduced lesion score to 2.9±0.05 and infected untreated groups revealed higher lesion (3.3±0.17). Most lesions in the TLZ-NPs group were sorted under score one, which described as follows: few scattered petechiae, no thickening of the cecal wall, cecal contents usually showing a normal brownish color, and no loss in the longitudinal cecal corrugation as classified (Fig. 6c).

Microscopic scoring of cecal tissue: Fig. 7a shows the normal histological structure of the negative control group, which indicates that no infection occurred. The infected group showed severe damage of villi enterocytes, which was completely sloughed in frequent areas (Fig. 7b). There was an obvious increase in lamina propria thickness due to the large infiltration of inflammatory cells. Congestion and severe hemorrhages were observed. Parasitic stages of Eimeria (meronts, gamonts, and schizonts) were observed in almost all epithelial cells in villi and crypts. In the Nalcoxi group, damage was observed in some areas of the intestinal lining expressing less edema and cellular infiltration. In the TLZ-NPs group, the epithelial lining was almost normal in most fields under evaluation (Fig. 7c). Few parasitic stages were observed in enterocytes in the TLZ-NPs group. They were also shrunken and disfigured (Fig. 7d). The cecal health index of each group, as evidenced by the ISI methodology, was compiled in Table (3). The infected-untreated group showed a higher maximum score (49) compared with the Nalcoxi (45) and the TLZ-NPs group (22) (P<0.05). This higher score was due to the increase of inflammatory cells, hemorrhages, and the presence of parasitic stages. The TLZ-NPs group represented the lowest maximum score (22) (Table 3).

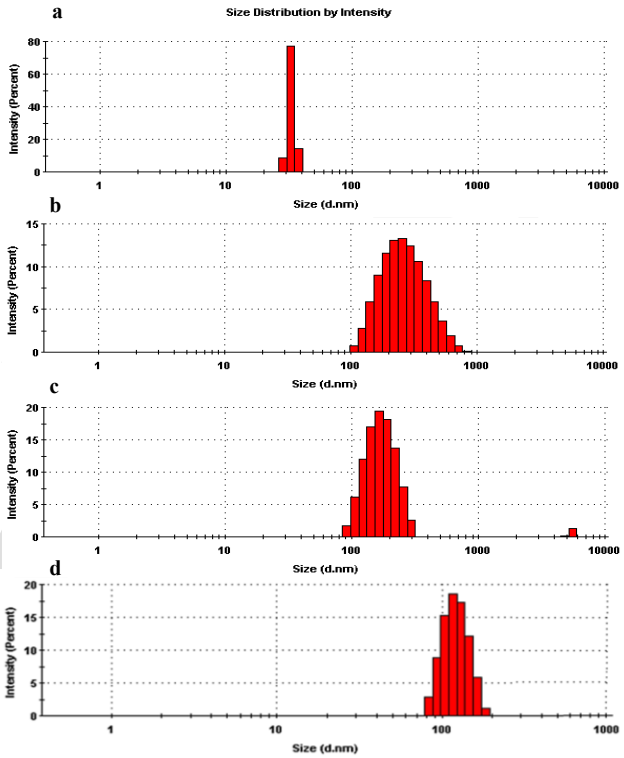

Fig. 2: Histograms of particle size distribution using the Malvern Zeta analyzer. a) Tween 1% stabilized toltrazuril nanoparticles (TLZ-NPs) represented an average size of 33.04 nm and poly dispersity index (PDI). b) NaDC 0.5% stabilized TLZ-NPs represented 243.1 nm average size and 0.1 PDI. c) Span 0.5% stabilized TLZ-NPs represented an average size of 173.5 nm and 0.2 PDI. d) Triton X100 0.5% stabilized TLZ-NPs represented 121.5 nm average size and 0.3 PDI. (Instillation speed was 50 µL/min and drug concentration was 0.17 mg/ml.).

Table 3: The microscopic alterations of the cecal tissue after treatment with commercial TLZ and TLZ-NPs compared with ISI at 7 days post infection.

Cecal tissue	Infected-untreated group		TLZ-NPs treated group		TLZ treated group	
	OIF score	Maximum	OIF score	Maximum	OIF score	Maximum
Lamina propria thickness	2		1		2	
Epithelial thickness	3		1		3	
Enterocytes proliferation	3		1		2	
Lamina propria inflammatory cell infiltration	2	49[a]	1	22[c]	2	45[b]
Goblet cell proliferation	3		1		3	
Haemorrhage	1		2		2	
Presence of parasitic stages	3		1		3	

Values with different superscripted letters [(a-c)] point to a significant difference (P<0.05).

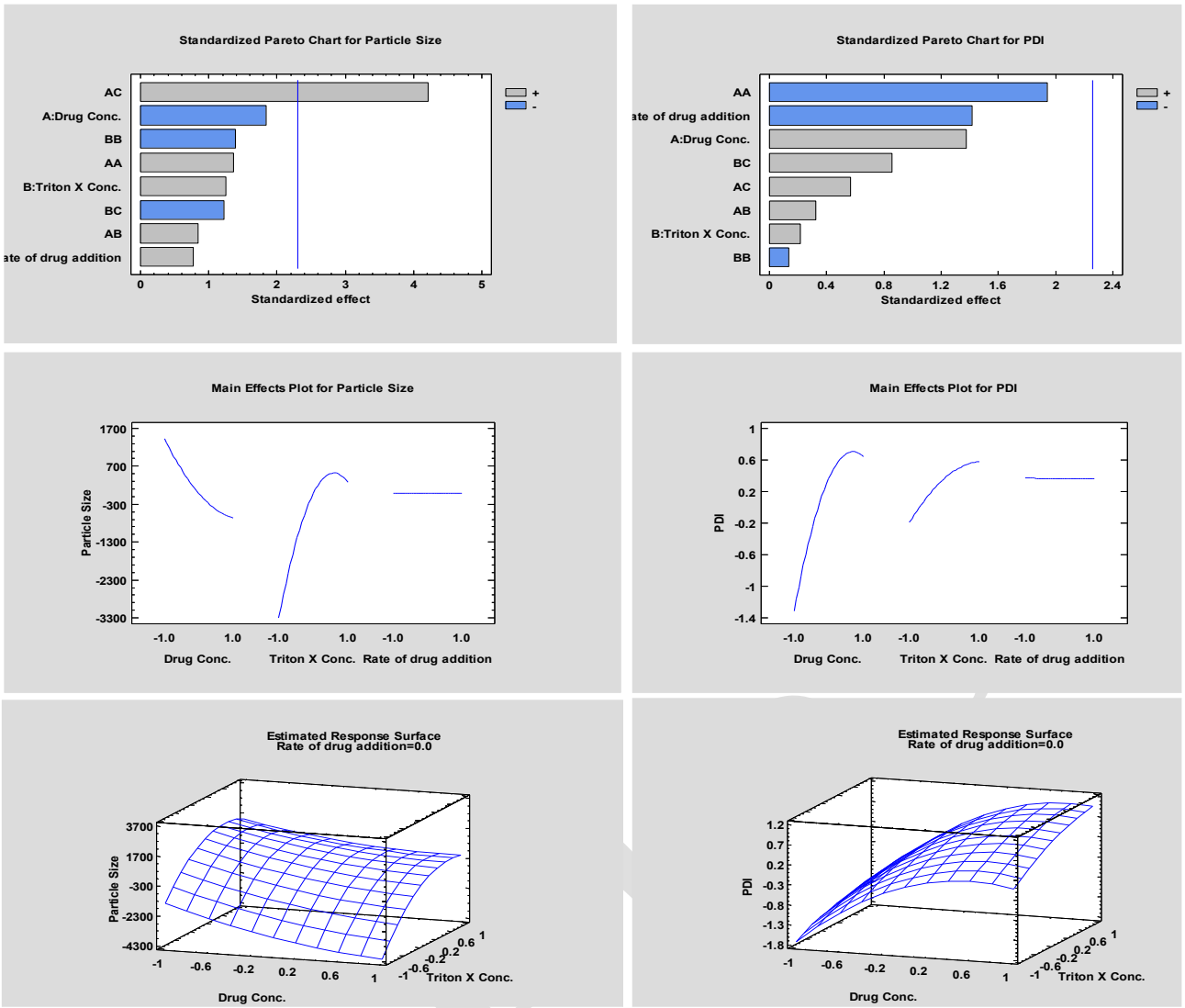

Fig. 3: The effect of triton X concentration in the toltrazuril nanoparticles **(**TLZ-NPs) based on multi-level full factorial design by Statgraphics XVII-X64 software; **a**) Standardized Pareto charts for the effect of studied factors on particle size and poly dispersity index (PDI). **b**) The main effects plot for particle size and PDI. **c**) 3D response surface plots estimating the effect of drug concentration and triton X concentrations on particle size and PDI.

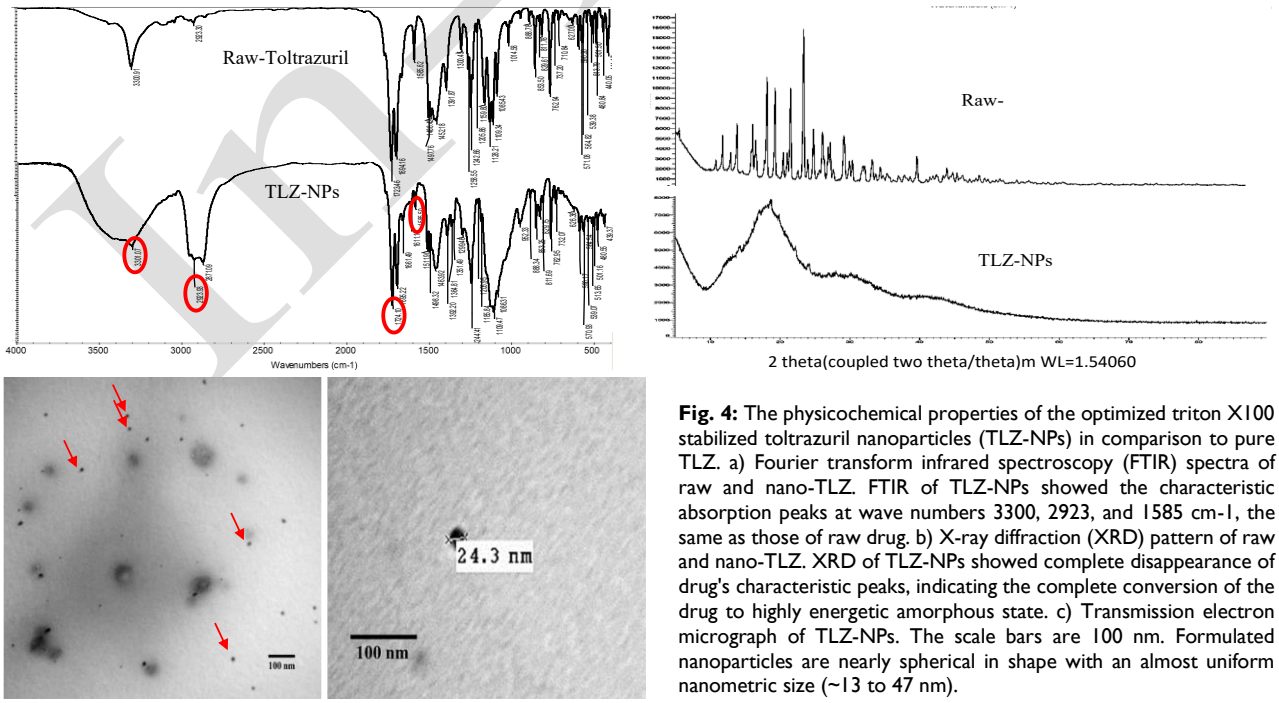

Fig. 4: The physicochemical properties of the optimized triton X100 stabilized toltrazuril nanoparticles (TLZ-NPs) in comparison to pure TLZ. a) Fourier transform infrared spectroscopy (FTIR) spectra of raw and nano-TLZ. FTIR of TLZ-NPs showed the characteristic absorption peaks at wave numbers 3300, 2923, and 1585 cm-1, the same as those of raw drug. b) X-ray diffraction (XRD) pattern of raw and nano-TLZ. XRD of TLZ-NPs showed complete disappearance of drug's characteristic peaks, indicating the complete conversion of the drug to highly energetic amorphous state. c) Transmission electron micrograph of TLZ-NPs. The scale bars are 100 nm. Formulated nanoparticles are nearly spherical in shape with an almost uniform nanometric size (~13 to 47 nm).

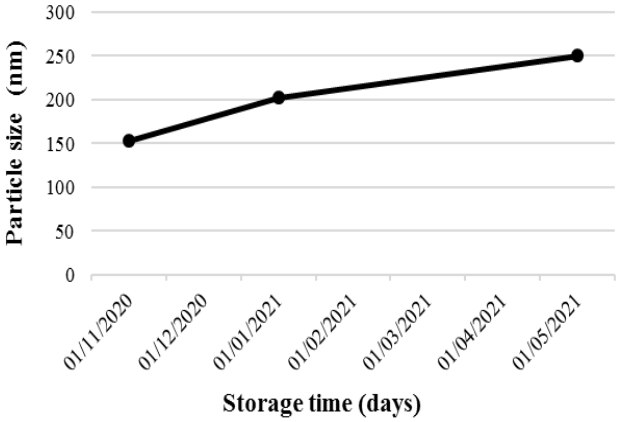

Fig. 5: Particle size distribution of triton x100 (0.5%) stabilized toltrazuril nanoparticles (TLZ-NPs) prepared by the solvent anti-solvent method (50 µl/min). Samples were stored in a dark container at 28 -32°C with RH (60 - 65%), over 7 months. Agitation was applied before pipetting for quantification. Values represent mean ± SD (n=3).

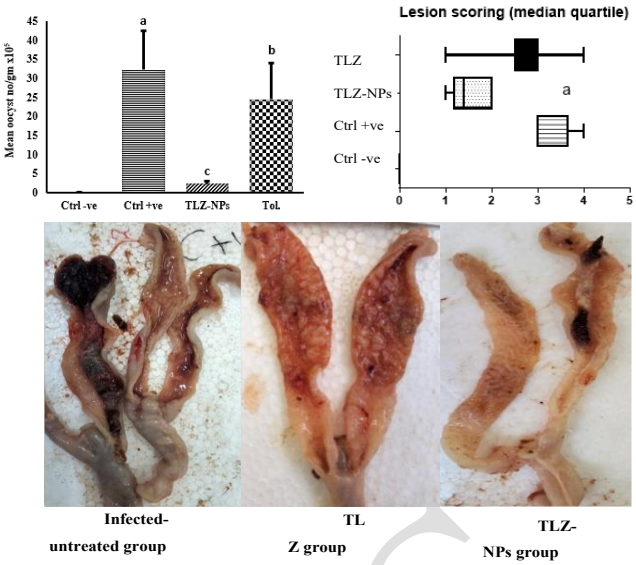

Fig. 6: The anticoccidial efficacy of toltrazuril nanoparticles (TLZ-NPs) in broiler chickens against *Eimeria tenella.* in comparison to commercial toltrazuril. **a**) Mean oocyst number per gram of cecal content in each group. The complete cecum contents of each bird were pooled separately, and oocysts were counted from 1 g of the feces ;**b**) Median quartiles of the mean cecal lesion scores in each group; **c**) Pathological changes in the cecal mucosa; Score lesion (~3.3±0.17) in infected-untreated group (left), score lesion (~2.9±0.05) in toltrazuril treated group (middle), Score lesion (~1.4±0.01) from nano-toltrazuril treated group (right).

DISCUSSION

Coccidiosis, a protozoan disease caused by *Eimeria* species, constitutes a significant problem for poultry farms worldwide. Although multiple anti-coccidial drugs and different types of vaccines have been used for disease management, their efficiency has been hindered by

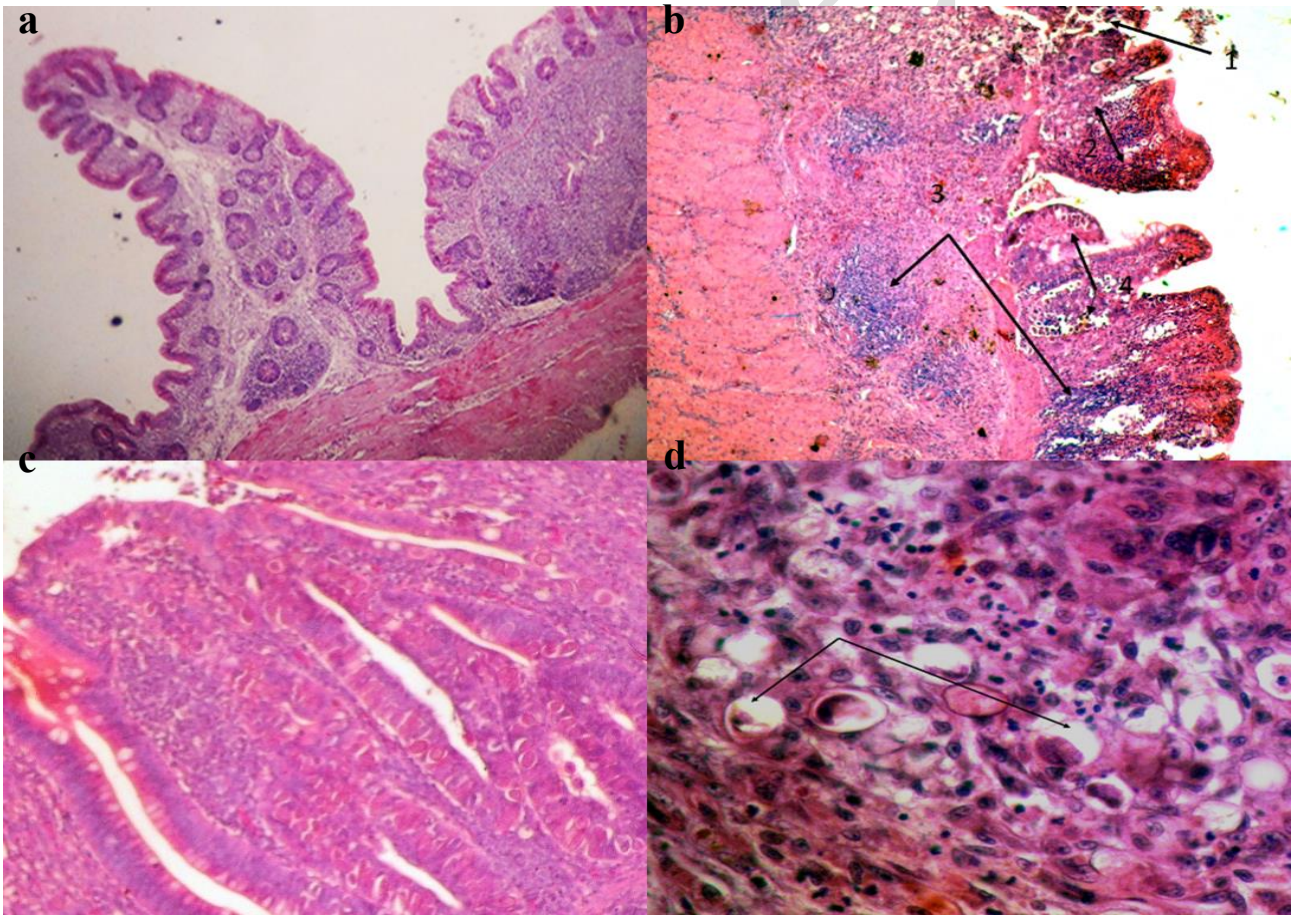

Fig. 7: Hematoxylin and eosin-stained histomicrograph of cecal tissue sections from the experimental chickens. **a**) Normal histological structure of the negative control group (200X); **b**) sloughing of the epithelial layer (arrow 1), increase in lamina propria thickness (arrow 2); Inflammatory cell infiltration (arrow 3); presence of parasitic stages (arrow 4) in the infected untreated birds, 200X; **c**) In the commercial TLZ-treated group the severity of lesions was less than in the infected unmedicated group. Some areas showed a lower level of mucosal damage, cellular infiltration, or presence of parasitic stages, 200X; **d**) The few parasitic stages observed in the TLZ-NPs treated group were shrunken in size and seemed to be disfigured and deteriorated, 400X.

several challenges such as costs, drugs residues and emerging of drug resistance (Mustafa *et al.,* 2025). The increased consumer demand for drug-free poultry meat raises interest in phytotherapeutics like essential oils and herbal extracts for avian coccidiosis. Essential oil of *Amomum subulatum* proved anticoccidial effects in the broiler chicks and has positive effects on the performance parameters (Saeed *et al.,* 2023). *Linum usitatissimum* extract reported for its anticoccidial activity (Hussain *et al.,* 2024). Recent advancements in nano-formulation have introduced new alternatives for combating coccidiosis, particularly using metal and metallic oxide nanoparticles (Dkhil *et al.*, 2015; Dkhil and Quraishy, 2016; Harron, *et al.,* 2024). These nanoparticles improve therapeutic efficacy when combined with anticoccidial drugs, offering better results.(Chauke and Siebrits 2012). Green nanotechnology has further refined treatment outcomes by decreasing toxicity while elevating effectiveness. Green-synthesized iron-oxide nanoparticles using *Ficus racemosa* Linn leaf extract enhanced recovery and growth performance in broilers infected with *E. tenella* (Khan *et al.,* 2023). Nanotechnology also offers a reformulation for chemotherapeutic drugs enhancing therapeutic potentials while reducing costs and improving safety profiles (El-Sawah *et al.,* 2024). With minimum resistance reported against it, the triazinetrione family is intensively used against coccidiosis in both mammals and poultry. The ability of toltrazuril to directly kill all lifecycle stages of *Eimeria spp*. was linked to three possible mechanisms. Firstly, it can halt asexual and sexual development (Harder and Haberkorn 1989) by suppressing mitochondria and the endoplasmatic reticulum (Jöckel *et al.*, 1998). Secondly, it was reported to inhibit nucleic acid synthesis enzymes like those responsible for pyrimidine synthesis and cell respiratory enzymes (Mehlhorn *et al*, 1988). A third possible technique is the prevention of nuclear division in schizonts and microgamonts and the suppression of wall-forming bodies Mehlhorn *et al*, 1984. All previous mechanisms were associated with using high drug concentrations (Harder and Haberkorn 1989). Triazinetrione family is poorly soluble in water. The drug usually precipitates, leading to poor gut absorption. During drug manufacture, some organic solvents are used to increase its solubility. The low safety margins of using these solvents limit the ability to use high concentrations of toltrazuril in commercial drugs. Therefore, different studies tried to form soluble solid dispersion (Haixia and Suying 2013), cyclodextrin inclusion complex (Lu *et al.,* 2012), or nano-emulsion (Zhang *et al.,* 2018) to increase the concentration of the drug in aquas solution. The utility of high-viscosity carriers such as polyethylene glycol and propylene glycol in new formulations leads to the accumulation of precipitate in the drinking system. In the present study, complete conversion of the drug from a low-energetic-crystalline state to a high-energetic amorphous state exhibited excellent solubility. The high aqueous solubility of the drug will be accompanied by high bioavailability, high plasma concentration, and therapeutic efficacy. High toltrazuril concentrations in the blood increased its ability to penetrate tissues and organs and reach in an abundant concentration in the intracellular stages of *Eimeria spp*. TLZ-NPs prominently reduced oocysts output less than the reference drug dose. Improving drug solubility and bioavailability will help reduce dosages and enhance efficiency, which will reduce overall costs. This formula can be adapted for large-scale production. Additionally, new drug formulation will decrease the residues and increase therapeutic outcomes, ultimately maximizing economic returns (Mesa-Pineda *et al.,* 2021; El-Sawah *et al.,* 2024). A previous trial using toltrazuril-loaded polymeric nanoparticles (NCt) or poly-"-caprolactone (LNCt) in drinking water reduced the lesion scores and oocysts shedding to a level similar to commercial drug (Baycox®, 7 mg/kg/day) (Baron *et al.,* 2022). Shedding reduction in the present study may be linked to several factors. The formula that was chosen to be evaluated in vivo consisted of 0.17 mg/ml toltrazuril with 0.5% triton X-100 and an average particle size of 152.7 nm. The TLZ-NPs contents were close to 100%, and the entrapment efficiency was more than 90%. Triton X can attach to epithelial cells and affect drug cell mobility. This can be achieved by prolonging the time when the tight junction between enterocytes is opened. Thereby, it increases the permeability of drug (Wu *et al.,* 2022). Moreover, Triton X-100 can increase oral absorption and decrease P-glycoprotein activity (Nguyen *et al.,* 2025). The TLZ-NPs enhances muco-adhesion, prolonging contact time with intestinal villi and increasing drug exposure time to Eimeria-infected tissues, further boosting treatment (El-Sawah *et al.,* 2024). The TLZ-NPs improve miscibility with gut content, ensuring uniform drug distribution. It enhances hydrophilic-lipophilic balance (HLB), allowing the drug to integrate seamlessly with different intestinal contents (aqueous mucus, lipids, and digesta). This hinders phase separation and ensures consistent drug availability across the entire gastrointestinal tract (Ahmed *et al.,* 2021). Modifying the physicochemical characteristics can also boost its effectiveness against strains of *Eimeria spp.* that exhibit resistance. In the current study, field isolate was used to test the efficacy of Nalcoxi and TLZ-NPs. The efficacy reduction of the reference drug dose of toltrazuril against infection has been reported in several studies (Lan *et al.,* 2017; Zhang *et al.,* 2019), and in Egypt as well (Harfoush *et al.,* 2010).

The efficiency of TLZ-NPs was more obvious in macroscopic and microscopic scoring. *Eimeria tenella* destroys the intestinal villi, leading to a reduction in absorption ability (Choi *et al.,* 2021). These protozoans initiate a local inflammatory response by developing inside the enterocytes (Tomal *et al.,* 2023), which leads to cellular explosion, edema, and epithelial sloughing. Microscopic examination of the cecum showed an increase in lamina propria thickness and inflammatory cell infiltration. Both parameters were used (Belote *et al.*, 2019) as good indicators to compare intestinal efficiency between different treatments. Reduction of ISI lined up to decrease intestinal absorption and birds' performance (Belote *et al.*, 2019). Cecal wall bleeding was detected in all challenged groups. While wall thickness usually follows due to severe destruction occurring in epithelial cells, minor inflammation was observed in TLZ-NPs. The administration of TLZ-NPs reduced the lesion significantly to a score of 1.4 with no actual functional damage observed. Nalcoxi induced a markedly higher lesion score in comparison to TLZ-NPs, although it still able to improve the lesion score. These results were also recorded for

Eudragit® S100 (NCt) or poly-caprolactone (LNCt) but, with these formulas, only half of toltrazuril concentration achieved results similar to those obtained by commercial drug (Baron *et al.,* 2022). The ability of the TLZ-NPs to penetrate the enterocytes and inhibit schizogony and merogony, markedly decreased the damaging effect of those stages' propagation.

In the challenged group, gut damage was more evident due to the high number of meronts infecting enterocytes. These stages explode the enterocytes to release merozoites in the intestinal lumen (Mesa-Pineda *et al.*, 2021). The more stages mature in enterocytes or submucosa, the more damage to intestinal wall (Burrell et al., 2020).

Few parasitic stages were observed in the enterocytes of the TLZ-NPs group, and most of them were degenerated and contained a lot of vacuolation. This is usually what cellular forms exhibit when protozoal cells die after being treated with antiparasitic agents (Taylor *et al*, 2003; Yuan *et al.*, 2024; Fathy *et al.,* 2024) . Nuclear division and cellular membrane disruption occur in most lifecycle stages, resulting in disfigured dead cells. The inflammatory cell infiltration as well as enterocyte damage markedly decreased in Nalcoxi in comparison to the challenged untreated group, which exhibit a marvelous number of parasitic stages.

Coccidial infection reduces the density of goblet cells in the intestine. In the present study, the challenge dose reduced about 50% of the goblet cells amount in non-treated chickens. The early treatment with TLZ-NPs prevented the reduction in goblet cells significantly. A similar finding was observed (Baron *et al.*, 2022, El sawah *et al.*, 2024). Efficient treatment of coccidiosis is not as simple as killing parasitic stages. The ideal treatment for coccidiosis should be able to reduce postmortem lesions, minimize oocysts shedding, and allow few stages to escape and propagate to induce cellular solid immunity (Taylor *et al,*2003). TLZ-NPs allow a few stages to be propagated in a similar way as the live vaccine does, which explains the few inflammatory responses observed in TLZ-NPs. This adds to its advantage in preventing heavy, damaging infection, and allow trickle infection to occur and initiate immunity. The introduced formula proved efficient, with a very low dose of toltrazuril equal to about 14% of the original commercial concentration. The ability of nano-formulation to reduce drug dose was the main target for many studies and has proven successful (Tang *et al.,* 2016). For such biodegradable and biocompatible drug, nano-formulation can be safely used without worry about drug residues either in meat or in excreta to environment.

Conclusions: In the present research, toltrazuril has been successfully formulated into a highly energetic amorphous form and developed excellent solubility. The increased aqueous solubility has resulted in significantly better potential benefits. TLZ-NPs recorded a better survival rate than other groups. TLZ-NPs significantly decreased oocysts output less than the reference drug dose. It effectively diminished the lesion score in intestinal tissues, with no actual structural damage observed. Few parasitic stages were observed in TLZ-NPs-treated intestinal cells, the majority of which disintegrated and showed a lot of cell shrinkage. The introduced formula has proven successful, with a very low dose of toltrazuril equivalent to about 14 percent of the original reference concentration. The cecal health index of each group, as detailed by the ISI methodology, the TLZ-NPs group (ISI=22) has less than the infected-untreated group (ISI=49) and the Nalcoxi treated group (ISI=45). By utilizing a lower concentration of raw material of toltrazuril, drug producers can significantly reduce the costs while get better efficiency. By using a lower concentration of the active materials of the drug, manufacturers can significantly reduce production costs while maintaining therapeutic efficacy. This will also help in reducing the risk of parasites developing resistance to the new formula, keeping the efficiency of toltrazuril for long-term veterinary needs.

Authors' contributions: Asmaa Nasr performed the experiments, analyzed the data and wrote the paper. Shiem El-Sherry designed, supervised, and coordinated the study, evaluated the performance and laboratory measurements, analyzed and interpreted the biological data, and drafted the manuscript. Gamal Zayed supervised the nano formulation, characterization, and interpretation of the results. All authors read and approved the final manuscript. Ethics approval and consent to participate.

All experiments were performed in experimental units of Avian and Rabbit Medicine Department, Faculty of Veterinary Medicine, Assiut University approved by The National Ethical Committee of The Faculty of Veterinary Medicine, Assiut University, Assiut, Egypt, according to The OIE standards for use of animals in research in accordance with ARRIVE guidelines. (certified no.06-2023-0030).

Competing interests: All authors declare that they have no competing interests.

REFERENCES

Ahmad SU, Li B, Sun J *et al.*, 2021. Recent advances in microencapsulation of drugs for veterinary applications. J Vet Pharmacol Ther 44(3):298-312.

Ahmed S, Ahmad M, Swami BL *et al.*, 2016. Green synthesis of silver nanoparticles using Azadirachta indica aqueous leaf extract. J Radiat Res Appl Sci 9(1):1-7 .

Baron LF, Fonseca FN, Maciag SS *et al.*, 2022. Toltrazuril-Loaded Polymeric Nanocapsules as a Promising Approach for the Preventive Control of Coccidiosis in Poultry. Pharmaceutics 14(2):392.

Belote BL, Soares I, Tujimoto-Silva A *et al.*, 2019. Applying I see inside histological methodology to evaluate gut health in broilers challenged with Eimeria. Vet Parasitol 276:100004.

Blake DP, Knox J, Dehaeck B *et al.*, 2020. Re-calculating the cost of coccidiosis in chickens. Vet Res 51(1):1-14 .

Burrell A, Tomley FM, Vaughan S *et al.*, 2020. Life cycle stages, specific organelles and invasion mechanisms of Eimeria species. Parasitology 147(3):263-278.

Chauke N and Siebrits FK, 2012. Evaluation of silver nanoparticles as a possible coccidiostat in broiler production. S Afr J Anim Sci 42(5):493-7 .

Choi J, Ko H and Tompkins Y, 2021. Effects of *Eimeria tenella* infection on key parameters for feed efficiency in broiler chickens. Animals 11(12):3428.

Dkhil MA and Al-Quraishy S 2016. Nanoparticles Against Eimeriosis. In: Nanoparticles in the Fight Against Parasites (pp. 207-210). Cham: Springer International Publishing. https://link.springer.com/chapter/10.1007/978-3-319-25292-6_11

Dkhil MA, Al-Quraishy S and Wahab R, 2015. Anticoccidial and antioxidant activities of zinc oxide nanoparticles on *Eimeria papillata*-induced infection in the jejunum. Int J Nanomed 10:1961.

El-Feky GS, Zayed G and Farrag ARH, 2013. Optimization of an ocular nanosuspension formulation for acyclovir using factorial design. Int J Pharm Sci 5(1):213-9 .

El-Sawah AA, Aboelhadid SM, El-Nahass ESN *et al*., 2024. Efficacy and safety of diclazuril nanoemulsion in control of *Eimeria tenella* in broilers. BMC Vet Res 20(1):495.

El-Sherry S, Ogedengbe ME, Hafeez MA *et al*., 2019. Cecal coccidiosis in turkeys: Comparative biology of Eimeria species in the lower intestinal tract of turkeys using genetically typed, single oocyst–derived lines. Parasitol Res 118(2):583-98.

Fathy G, Farah K, El-hamied SS et al, 2023. Evaluation of the effects of diclazuril and toltrazuril on hematological changes, antioxidant status immune response and cecal histoarchitecture of chickens experimentally infected with *Eimeria tenella*. Benha Vet Med J 45(2):71-76.

Haixia L and Suying M, 2013. Preparation and characterization of toltrazuril polyethyleneglycol 6000 solid dispersions with improved solubility. Afr J Pharm Pharmacol 7(8):450-3 .

Harder A and Haberkorn A, 1989. Possible mode of action of toltrazuril: studies on two Eimeria species and mammalian and Ascaris suum enzymes. Parasitol Res 76(1):8-12 .

Harfoush MA, Hegazy AM, Soliman AH *et al*., 2010. Drug resistance evaluation of some commonly used anti-coccidial drugs in broiler chickens. J Egypt Soc Parasitol agosto de 40(2):337-348 .

Holdsworth PA, Conway DP, McKenzie ME *et al*., 2004 World Association for the Advancement of Veterinary Parasitology (WAAVP) guidelines for evaluating the efficacy of anticoccidial drugs in chickens and turkeys. Vet Parasitol 121(3-4):189-212 .

Hussain k, Abbas A, Rehman A *et al*., 2024. Evaluating Linum usitatissimum Seeds Extract as Potential Alternative Biochemical and Therapeutic Agent Against Induced Coccidiosis in Broiler Chicken. Kafkas Univ Vet Fak Derg 30.(6)

Jöckel J, Wendt B and Löffler M, 1998. Structural and functional comparison of agents interfering with dihydroorotate, succinate and NADH oxidation of rat liver mitochondria. Biochem Pharmacol 56(8):1053-60 .

Khan A, Afzal M, Rasool K *et al*., 2023. In-vivo anticoccidial efficacy of green synthesized iron-oxide nanoparticles using Ficus racemosa Linn leaf extract. (Moraceae) against *Emeria tenella* infection in broiler chicks. Vet Parasitol 321:110003.

Kraieski AL, Hayashi RM, Sanches A *et al*., 2017. Effect of aflatoxin experimental ingestion and Eimeira vaccine challenges on intestinal histopathology and immune cellular dynamic of broilers: applying an Intestinal Health Index. Poul Sci 96(5):1078-1087.

Lan LH, Sun BB, Zuo BXZ, Chen XQ *et al*., 2017. Prevalence and drug resistance of avian Eimeria species in broiler chicken farms of Zhejiang province, China. Poult Sci 96(7):2104-9 .

Lee BH, Kim WH, Jeong J *et al*., 2010. Prevalence and cross-immunity of Eimeria species on Korean chicken farms. J Vet Med Sci 72(8):985-9 .

Li M, Lv X, Zheng M *et al*., 2023. The Immunoprotective Effect of ROP27 Protein of *Eimeria tenella*. Animals 13(22)3500 .

Lu CC, Yang J and Zhang W, 2012. Preparation and characterization of toltrazuril–hydroxypropyl-β-cyclodextrin inclusion complex. J Process Eng 12(6):982-8.

Mehlhorn H, Schmahl G and Haberkorn A, 1988. Toltrazuril is effective against a broad spectrum of protozoan parasites. Parasitol Res 75(1):64-6 .

Mehlhorn H, Ortmann-Falkenstein G and Haberkorn A, 1984. The effects of sym. triazinetriones on developmental stages of *Eimeria tenella*, E. maxima and *E. acervulina*: a light and electron microscopical study. Z Parasitenkd 70(2):173-82 .

Mesa-Pineda C, Navarro-Ruíz JL, López-Osorio S *et al*., 2021. Chicken Coccidiosis: From the Parasite Lifecycle to Control of the Disease. Front Vet Sci 8:787653 .

Mustafa S, Abbas RZ, Saeed Z, *et al*., 2025. Use of Metallic Nanoparticles Against Eimeria: the Coccidiosis-Causing Agents: A Comprehensive Review: Biol Trace Elem Res 203(6):3412-3431 .

Nguyen TTL, Duong VA and Maeng HJ, 2021. Pharmaceutical formulations with P-glycoprotein inhibitory effect as promising approaches for enhancing oral drug absorption and bioavailability. Pharmaceutics 13(7):1103.

Pouretedal HR, 2014. Preparation and characterization of azithromycin nanodrug using solvent/antisolvent method. Int Nano Lett 4(1):1-9.

Saeed Z, Abbas RZ, Khan MK *et al*., 2023. Anticoccidial activities of essential oil of *Amomum subulatum* in broiler chicks. Pak J Agric Sci 60:2.

Sun H, Su X, Fu Y *et al*., 2023. Pathogenicity and drug resistance of the *Eimeria tenella* isolate from Yiwu, Zhejiang province, eastern China. Poult Sci 102(8):102845.

Tang J, Zhang L, Gao H *et al*., 2016. Co-delivery of doxorubicin and P-gp inhibitor by a reduction-sensitive liposome to overcome multidrug resistance, enhance anti-tumor efficiency and reduce toxicity. Drug Deliv 23(4):1130-43 .

Taylor MA, Catchpole J, Marshall J *et al*., 2003. Histopathological observations on the activity of diclazuril (Vecoxan®) against the endogenous stages of *Eimeria crandallis* in sheep. Vet Parasitol 116(4):305-14 .

Tomal F, Sadrin G, Gaboriaud P *et al*., 2023. The caecal microbiota promotes the acute inflammatory response and the loss of the intestinal barrier integrity during severe Eimeria tenella infection. Front cell Infect Microbiol 13:1250080.

Yuan Y, Zhao Q, Xiong L *et al*., 2024. Ponazuril: Clinical efficacy, ultrastructure, and histopathology studies of in vivo anticoccidial action against *Eimeria tenella*. Vet Parasitol 326:110098 .

Wu CY and Wang W, 2022. Application of Antisolvent Precipitation Method for Formulating Excipient-Free Nanoparticles of Psychotropic Drugs. Pharmaceutics 14(4):819 .

Zaheer T, Abbas RZ, Imran M *et al*., 2022. Vaccines against chicken coccidiosis with particular reference to previous decade: progress, challenges, and opportunities. Parasitol Res 121(10):2749-2763 .

Zhang M, Li X, Zhao Q *et al*., 2019. Anticoccidial activity of novel triazine compounds in broiler chickens. Vet Parasitol 267:4-8 .

Zhang L, Ren D, Zhou J *et al*., 2018. Toltrazuril mixed nanomicelle delivery system based on sodium deoxycholate–Brij C20 polyethylene ether–triton x100: Characterization, solubility, and bioavailability study. Colloids Surf B Biointerfaces 163:125-32.